Agonist binding of human mu opioid receptors expressed in the yeast Pichia pastoris: Effect of cholesterol complementation

Franck Talmont, Chantal Lebrun, Jean-Marie Zajac

Agonist binding of human mu opioid receptors expressed in the yeast *Pichia pastoris:* effect of cholesterol complementation

Franck Talmont[a,b] , Chantal Lebrun[c] and Jean-Marie Zajac[a,b]

[a]Centre National de la Recherche Scientifique, Institut de Pharmacologie et de Biologie Structurale, F-31077 Toulouse, France

[b]Université de Toulouse, Université Paul Sabatier, Institut de Pharmacologie et de Biologie Structurale, F-31077 Toulouse, France

[c]INTHERES, UMR 1331 TOXALIM - BP 93173 F-31027 TOULOUSE Cedex 3, France

Correspondence should be addressed to F. T. (franck.talmont@ipbs.fr)

Keywords

GPCR; G protein coupled receptor; mu opioid receptor; cholesterol; ergosterol, Pichia pastoris; pharmacology, neuropeptide

Abstract

This study compared pharmacological profiles between human mu opioid receptors (hMOR) overexpressed in the SH-SY5Y neuroblastoma cell line (SH-hMOR) and the methylotrophic yeast *Pichia pastoris* (Pp-hMOR). Affinity determinations were performed by direct binding with the tritiated agonist DAMGO and antagonist diprenorphine (DIP). Additionally, displacement of these drugs with agonists (morphine and DAMGO) and antagonists (β-funaltrexamine, naloxone and diprenorphine) was examined. Tritiated DAMGO could bind to membranes prepared from Pp-hMOR, although the receptor was not coupled with G-proteins. The data obtained with this yeast strain suggested that only 7.5% of receptors were in a high-affinity-state conformation. This value was markedly less than that estimated in SH-hMOR membranes, which reached 50%. Finally, to understand the pharmacological discrepancies between Pp-hMOR and SH-hMOR, the role of sterols was evaluated. The major sterol in *P. pastoris* is ergosterol, while hMOR naturally functions in a cholesterol-containing membrane environment. Cell membranes were sterol-depleted or cholesterol-loaded with methyl-β-cyclodextrine. The results indicated that cholesterol must be present to ensure Pp-hMOR function. The proportion of high-affinity-state conformation was reversibly increased by cholesterol complementation.

1. Introduction

The methylotrophic yeast *Pichia pastoris* is a host of choice for the recombinant expression of G-protein coupled receptors (GPCR) (Sarramegna, Talmont et al. 2003; Bertheleme, Singh et al. 2015; Hartmann, Kugler et al. 2016). This particular class of transmembrane proteins is involved in many biological processes and is thus implicated in many diseases, including cancer, cardiovascular, inflammatory and metabolic diseases (Hutchings, Koglin et al. 2010). During drug design, an increasing number of GPCR 3-dimensional (3-D) structures have been determined using X-ray methods (Thal, Vuckovic et al. 2018). Among these 3-D structures, histamine H1 (Shimamura, Shiroishi et al. 2011) and adenosine A2A (Hino, Arakawa et al. 2012) receptors structures were obtained using *P. pastoris* as the host for recombinant protein expression. In general, host choice for recombinant receptor production is a function of the expression level and ability to crystallise rather than a function of pharmacological profiles. *P. pastoris* combines the advantages of easy manipulation, rapid growth rate and low cost of protein production.

Opioid receptors are a GPCR superfamily that comprise four subtypes: mu, delta, kappa and nociceptin/orphanin FQ (N/OFQ). These receptors are implicated in pain perception and addiction processes. The mu opioid receptor (hMOR) is most studied because it binds to endogenous opioid peptides and opiate drugs such as morphine and heroin. Opioid receptor 3-D structures were resolved using *Spodoptera frugiperda* (Sf9) insect cells as an expression system. These findings have been important to decipher the fine activation and functioning of these membrane proteins at angstrom resolution (Granier, Manglik et al. 2012; Manglik, Kruse et al. 2012; Thompson, Liu et al. 2012; Wu, Wacker et al. 2012; Huang, Manglik et al. 2015;

Sounier, Mas et al. 2015). However, most recombinant receptors used to obtain 3D-structures were expressed with truncated and modified forms (e.g., incorporation of T4 lysozyme) or constrained with nanobodies (Salom, Padayatti et al. 2013; Thorsen, Matt et al. 2014; Huang, Manglik et al. 2015; Koehl, Hu et al. 2018). Few results on receptor pharmacology prior to or during solubilisation, purification and crystallisation (Manglik, Kruse et al. 2012; Huang, Manglik et al. 2015; Koehl, Hu et al. 2018) are provided. The severely modified mu opioid receptor that was crystallised in 2012 (Manglik, Kruse et al. 2012) was only characterised with the ligand diprenorphine (DIP), a non-selective antagonist at opioid receptors. This research is disappointing given the allosteric nature of GPCRs. One limit of the insect cell system as a choice for recombinant protein expression is that the conformations expressed in the sterol-free membrane of sf9 cells do not represent the *in vivo* functional folding states in their natural mammalian membrane environments. The most successful choice of host for the recombinant production of eukaryotic membrane receptors must compare the pharmacological behaviour of the recombinant and endogenous receptors.

The present study proposes a pharmacological characterisation of hMOR expressed in *P. pastoris* (Pp-hMOR). Previous studies demonstrated that the selective mu opioid receptor agonist [D-Ala^2, MePhe^4, Gly-ol^5]enkephalin (DAMGO) is unable to bind Pp-hMOR with nanomolar affinity (Talmont, Sidobre et al. 1996). We showed that uncoupling agents have no effect on agonist binding, data that reflect the lack of functional interactions of Pp-hMOR with host G-proteins (Talmont, Sidobre et al. 1996). Nevertheless, DAMGO can displace the antagonist DIP (Talmont, Sidobre et al. 1996; Wu and Wong 2005) and displays a low affinity for hMOR, as determined with displacement studies.

To better understand agonist versus antagonist binding of Pp-hMOR, we reinvestigated mu opioid receptor pharmacology in *P. pastoris.* The human SH-SY5Y neuroblastoma cell line, which is widely used in opioid pharmacology, was used to overexpress human mu opioid receptors (SH-hMOR) in its natural environment. The pharmacological profiles of Pp-hMOR and SH-hMOR were compared. In the first attempt, direct radioligand binding assay of agonists and antagonists were used to provide information on drug affinity and to determine the number of receptor sites labelled by each ligand in the tested concentration range. These results were performed with competition binding by displacing a radiolabelled ligand with the same free ligand. The interaction of Pp-hMOR and SH-hMOR with others agonists and antagonists was also examined by competition binding. Furthermore, because ergosterol is the principal fungal sterol while cholesterol is the major sterol found in animal cell membranes, the role of membrane sterol composition on agonist binding with Pp-hMOR was evaluated. We demonstrated that Pp-hMOR can bind pharmacologically relevant drugs in an ergosterol-containing environment. However, there was a significant reduction in the proportion of high-affinity-state conformations compared to our reference. Cholesterol must be present to recover natural binding parameters. Taken together, this work highlights an example of how opioid receptor function can be altered by environmental changes.

2. Materials and methods

2.1 Expression of human mu opioid receptors

The human mu opioid receptor was expressed in the SMD1163 (his4, pep4, prB1) *P. pastoris* strain (his4, pep4, prB1), as described previously (Sarramegna, Muller et al. 2005). Pp-hMOR growth and induction media were BMGY (1% [w/v] yeast extract, 2% [w/v] peptone, 0.1 M phosphate buffer pH 7.5, 1% [v/v] glycerol) and BMMY (same as BMGY except that glycerol was replaced by 1% [v/v] methanol), respectively. Induction of expression was performed for 48 h at 20°C in shacked flasks that contained 2% dimethylsulfphoxide (DMSO). SH-hMOR (Mouledous, Neasta et al. 2005) cells were cultured, until confluence, in Dulbecco's Modified Eagle's Medium supplemented with 10% foetal bovine serum, penicillin (100 U/mL), streptomycin (100 mg/mL) and geneticin (500 µg/mL) in a humidified atmosphere that contained 95% air and 5% CO_2 at 37°C.

2.2 Membrane preparation

All operations were performed at 4°C. For Pp-hMOR, after induction of expression, cells were harvested and broken for 30 min with glass beads in breaking buffer (10 mM Tris–HCl, pH 8) supplemented with protease inhibitors (1 µg/ml each of benzamidine, pepstatin A, leupeptin, antipain and aprotinin 1 µg/ml). The cell lysate was then centrifuged at 1,000 *g* for 15 min to remove unbroken cells and particulate matter. The supernatant was further centrifuged at 10,000 *g* and 100,000 *g* for 30 min each to harvest the total membrane fraction. For SH-hMOR, cells were broken in ice cold 50 mM Tris–HCl buffer (pH 7.4) with a Potter Elvehjem tissue grinder. A membrane fraction was obtained after centrifugation at 1,000 *g* for 15 min and

100,000 *g* for 30 min. The resulting pellets were then stored at -80°C in breakage buffer. Protein content was determined using the Bradford method.

2.3 Radioligand binding assays

Saturation binding assays were performed for 1 h at 25°C in 500 µl binding buffer (50 mM Tris-HCl, pH 7.5, 10 mM ethylenediaminetetraacetic acid [EDTA], 0.1% bovine serum albumin [BSA]) that contained cell membranes and varying concentrations of [^{3}H]-DIP (50 Ci/mmol, Perkin-Elmer) or [^{3}H]-DAMGO (50 Ci/mmol, Perkin-Elmer). Non-specific binding was determined in parallel test tubes in the presence of unlabelled DIP or DAMGO. Bound and free ligand were separated by rapid filtration on Whatman GF/B filters soaked in 0.3% polyethylenimine, and after three washes with 10 mM Tris-HCl (pH 7.5), filter-bound radioactivity was determined using a Packard scintillation counter. The measured data are presented in disintegrations per minute (dpm) or were converted to nmol per mg protein for specific activity. The conversion factor 1 Ci = 2.22 x 10^{12} dpm and the specific activity (Ci/mmol) of each isotope were used.

For displacement studies, various concentrations of unlabelled opioid ligands (morphine [MOR], naloxone [NAL], DIP, β-funaltrexamine [βFNA] and DAMGO) were used to displace 1 nM [^{3}H]-DIP or [^{3}H]-DAMGO. Data were analysed with GraphPad PRISM (GraphPad software, San Diego, USA), and the results are presented as the mean ± standard error of the mean (SEM) of three independent experiments performed in duplicate. One-hundred µM GTPγS was added in saturation and displacement assays.

2.4 [^{35}S]-GTPγS binding assay

Membranes were assayed in a final volume of 500 µl that contained 20 mM HEPES (pH 7.4), 100 mM NaCl, 3 mM $MgCl_2$, 10 µM GDP, 0.1% BSA and 5 µg saponin. Tubes were incubated for 60 min at 30°C with 0.1 nM [^{35}S]-GTPγS and various DAMGO concentrations.

2.5 Sterol depletion and complementation

To deplete sterols, Pp-hMOR cell membranes (1 mg/ml protein) were incubated with 20 mM methyl-β-cyclodextrin (MβCD) for 1 h at 20°C, with constant shaking, in 50 mM Tris-HCl (pH 7.4) buffer supplemented with protease inhibitors (Complete Mini, Roche). Suspensions were centrifuged at 110,000 *g* and washed with the same buffer for 20 min to remove MβCD. To load cholesterol in depleted membranes, fractions (1 mg/ml) were incubated for 30 min at 20°C under agitation with an equal volume of cholesterol–MβCD complexes and washed as described above. Controls were prepared with membranes that were obtained using the same protocol but with buffer that contained no MβCD or cholesterol–MβCD complexes. Cholesterol-MβCD complexes (1:9 molar ratio) were prepared by adding a solution of 8.6 mg cholesterol in 100 µl pure dimethylformamide dropwise to 10 ml of a 40 mM MβCD solution at 70°C, under agitation.

3. Results

3.1 Saturation binding assays

Pp-hMOR cell membranes were analysed for their ability to bind the agonist [^{3}H]-DAMGO and the antagonist [^{3}H]-DIP. To ascertain the acquisition of spotless specific binding curves, non-specific binding was performed with the non-radioactive ligand counterparts. Nonspecific binding relative to total binding represented 10-15% of the utilised ligand (Fig. 1). For Pp-hMOR, representative saturation curves for [^{3}H]-DAMGO and [^{3}H]-DIP are presented in Fig. 1. [^{3}H]-DAMGO saturation binding analysis revealed a K_D of 7.4 ± 1.5 nM and a Bmax of 0.031 ± 0.003 pmol/mg membrane protein (Table 1). Compared to [^{3}H]-DAMGO, the [^{3}H]-DIP K_D was 3-fold less (2.4 ± 0.3 nM) and the B_{max} value was 10-fold higher (0.4 ± 0.1 pmol/mg; Table 1). In SH-hMOR, K_D values for DAMGO and DIP were 1.06 ± 0.07 nM and 0.34 ± 0.07 nM, respectively (Talmont, Mouledous et al. 2014). The K_D (DAMGO):K_D (DIP) ratio was nearly 3 for hMOR in *P. pastoris* and SH-SY5Y cells, whereas the B_{max} (DIP):B_{max}(DAMGO) ratio was 2 in SH-SY5Y cells and 13 in *P. pastoris.* Thus, the number of *P. pastoris* receptors labelled by [^{3}H]-DAMGO was only 7.5% of the number of receptors labelled by [^{3}H]-DIP. This amount was markedly lower compared to the 50% in SH-SY5Y cells. If we consider that the binding values obtained in SH-hMOR cells represent the standard, we must concede that *P. pastoris* is unable to provide a proper environment for hMOR expression. Nevertheless, direct ligand binding parameters must be confirmed with displacement studies using various ligands.

3.2 Competition binding assays

A panel of opioid receptor agonists and antagonists was used to displace both [^{3}H]-DAMGO and [^{3}H]-DIP (Fig. 2; Table 2). For SH-hMOR, all ligands displaced [^{3}H]-DAMGO and [^{3}H]-DIP in the low nanomolar range. However, the same was not true for Pp-hMOR. Specifically, DAMGO, MOR and NAL induced displacement above 10 nM, data that suggest a lesser apparent affinity for these ligands. Displacing a radiolabelled ligand with the same free ligand (using the so-called homologous competition assay) enables evaluation of the effect of a radioisotope on binding and to test a wider concentration range. In *P. pastoris*, the displacement of [^{3}H]-DAMGO with DAMGO produced a Ki of 15.7 ± 2.3 nM, while the displacement of [^{3}H]-DIP with DIP led to a Ki of 3.1 ± 0.7 nM (Table 2). In SH-SY5Y cells, the Ki of [^{3}H]-DAMGO displacement with DAMGO was 0.7 ± 0.1 nM, and the Ki of [^{3}H]-DIP displacement with DIP was 0.12 ± 0.01 nM (Table 2). Thus, for both Pp-hMOR and SH-hMOR, the Ki values for DAMGO and DIP, measured by homologous competition binding, were similar to the K_D binding values of [^{3}H]-DAMGO and [^{3}H]-DIP, respectively (Tables 1 and 2). Displacing a radiolabelled ligand with another ligand allows one to characterise unlabelled ligand over a wide concentration range. For Pp-hMOR, displacement of [^{3}H]-DIP with DAMGO produced a higher apparent Ki of 107 ± 10 nM (Table 1) compared to the so-called homologous competition assay. The Ki values for DAMGO were comparable in the homologous or heterologous competition assays for SH-hMOR. For *P. pastoris*, to displace [^{3}H]-DIP (Fig. 2A), the rank order of potency was DIP > β-FNA > NAL > DAMGO = MOR (Table 2). For [^{3}H]-DAMGO (Fig. 2B), the rank order of potency was β-FNA > DIP > DAMGO > MOR > NAL (Table 2). In SH-hMOR, to displace [^{3}H]-DIP, the rank order of potency was DIP > β-FNA =

DAMGO = NAL > MOR (Fig. 2C); to displace [^{3}H]-DAMGO, the rank order of potency was DIP > β-FNA = DAMGO > NAL > MOR (Fig. 2D).

3.3 [^{35}S] GTPγS binding assay

[^{35}S]-GTPγS binding measurements were used to determine the ability of DAMGO to trigger G-protein activation. In SH-hMOR, [^{35}S]-GTPγS binding was stimulated with DAMGO with an agonist potency (EC50) value of 2.7 ± 0.5 nM (Talmont, Mouledous et al. 2014). However, a flat curve was obtained with Pp-hMOR (Fig 3A). This result indicated that DAMGO lacked the ability to stimulate [^{35}S]-GTPγS binding, a deficiency that was probably due to the inability of receptors to bind endogenous G-proteins.

3.4 Uncoupling of hMOR from G-proteins

In SH-hMOR membranes, the addition of GTPγS shifted the DAMGO dose-response curve to the right and reduced Bmax by 25% (Fig. 3D). This decrease in receptor affinity for agonist was confirmed with higher Ki values (Fig. 3B). In contrast, there was no effect on DAMGO saturation curves when GTPγS was added to *P. pastoris* samples (Fig. 3C).

3.5 Effect of sterol depletion and complementation on ligand affinity

MβCD was used to deplete *P. pastoris* membranes of sterols. This depletion affected the binding of neither [^{3}H]-DAMGO (K_D = 10.6 ± 1.4 nM; Table 3) nor [^{3}H]-DIP (data

not shown). Displacement of [^{3}H]-DAMGO with DAMGO (141 ± 68 nM) and displacement of [^{3}H]-DAMGO with MOR (133 ± 39 nM) showed a 3-to-4-fold decrease in affinity, but Bmax determined with [^{3}H]-DAMGO (Fig. 4) was unaffected. MβCD was also used to load cholesterol prior to and after sterol depletion. When cholesterol was loaded in sterol-depleted membranes, [^{3}H]-DAMGO (K_D = 4.6 ± 0.9 nM, Ki = 4.1 ± 1.5 nM) affinities increased (Table 3). Furthermore, the Ki value for morphine was restored (Ki = 31 ± 7 nM). Similarly, cholesterol-loaded membranes presented an increased DAMGO affinity and no change for morphine. These data suggested that MOR binding depended on the presence of sterol (ergosterol or cholesterol), whereas DAMGO binding required the presence of cholesterol in the membrane that expresses hMOR.

4. Discussion

In this study, pharmacological characterisation of Pp-hMOR and SH-hMOR were performed by direct binding with [^{3}H]-DAMGO, a mu-receptor-selective synthetic peptide agonist derived from an endogenous ligand, and [^{3}H]-DIP, a non-selective small molecule opioid receptor antagonist derived from morphine. The interaction of agonists and antagonists was also examined by competition of these tritiated radioligands with unlabelled DAMGO, DIP, MOR, β-FNA and NAL. MOR, an alkaloid extracted from opium, is a specific mu opioid agonist. β-FNA is a mu-selective antagonist, whereas NAL is a non-selective synthetic morphinan-derived opioid antagonist.

In the human SH-SY5Y neuroblastoma cell line that is widely used in opioid pharmacology, two of the three endogenous opioid receptors can interact with DIP. Given that the mu opioid receptor content is 300-fold higher in overexpressing compared to wild type cells, SH-hMOR is an excellent model to characterise hMOR (Talmont, Mouledous et al. 2014). Indeed, in SH-SY5Y, mu opioid receptors account for twice the amount of the delta type that also bind to DIP, whereas kappa opioid receptors are not present (Alt, Clark et al. 2002) and DIP does not bind to nociceptin receptors (Mollereau, Parmentier et al. 1994). For SH-hMOR, K_D values determined from saturation binding isotherms were 1.06 ± 0.07 nM and 0.34 ± 0.07 nM for [^{3}H]-DAMGO and [^{3}H]-DIP, respectively. These values were similar to the Ki values obtained using the so-called homologous competition assay (Ki for DIP displacing [^{3}H]-DIP or Ki for DAMGO displacing [^{3}H]-DAMGO). Thus, for all ligands, no matter the utilised radioligand, the K_i values were in the nanomolar range. These values

obtained in SH-hMOR are compatible with pharmacological values determined for endogenous mu opioid receptors. For example, specific binding of DAMGO to brain membranes of human subjects are approximately 1-2 nM (Gabilondo, Meana et al. 1994; Gabilondo, Meana et al. 1995). The wide array of variously sized molecules that can bind to receptors can be explained by the existence of a very large drug-binding cavity (610 to 930 $Å^3$) of the mu opioid receptor (Cui, Yeliseev et al. 2013).

In Pp-hMOR, the K_D constant for [^{3}H]-DIP was 2.4 ± 0.3 nM (Fig. 1; Table 1), which is close to the Ki values for DIP determined in the homologous competition assay (Tables 1 and 2). The same rank order of potency to displace [^{3}H]-DIP or [^{3}H]-DAMGO was retained for the antagonists. For [^{3}H]-DAMGO, the K_D constant was 7.4 ± 1.5 nM (Table 1), and the apparent Ki value for DAMGO, determined in the homologous competition assay, was 15.7 ± 2.3 nM (Table 2). MOR displayed a similar potency for displacing [^{3}H]-DAMGO (267 ± 7.0 nM; Table 2). On the contrary, significantly higher apparent Ki values (approximately 110 nM) were measured for DAMGO and MOR in the competition binding for the displacement of the antagonist [^{3}H]-DIP. In our first works on mu opioid receptors expressed in *P. pastoris* (Talmont, Sidobre et al. 1996; Sarramegna, Talmont et al. 2002; Sarramegna, Muller et al. 2005), we did not perform direct binding with [^{3}H]-DAMGO, in part because it was possible to assess Ki values by displacement of [^{3}H]-DIP and also because [^{3}H]-DAMGO did not display any direct binding on membranes from *Saccharomyces cerevisiae* that express hMOR (Sc-hMOR) (Gaibelet, Meilhoc et al. 1999; Lagane, Gaibelet et al. 2000). The ascomycetes *P. pastoris* and *S. cerevisiae*, have important phylogenetic, genetic and biochemical similarities (Suh, Blackwell et al. 2006; Darby, Cartwright et al. 2012). In our previous studies in *P. pastoris*, as in Sc-hMOR,

DAMGO displaces [^{3}H]-DIP (Ki = 90 ± 10 nM) (Gaibelet, Meilhoc et al. 1999). We concluded that hMOR presents only low-affinity-state conformations for agonists, an explanation that underscores it pharmacological behaviours (Talmont, Sidobre et al. 1996; Lagane, Gaibelet et al. 2000). In the present work, we showed that the receptor expressed in *P. pastoris* can bind both agonists and antagonists with nanomolar affinities but with a significant reduction in affinity compared to our reference.

On the other hand, the total number of receptors estimated by the B_{max} value measured in the saturation binding experiments varied with the choice of ligand. In Pp-hMOR**,** the B_{max} (DAMGO):B_{max} (DIP) ratio was 1:13 ratio, compared to 1:2 in SH-hMOR. The same ratio was observed when hMOR was expressed in HEK cells (Cui, Yeliseev et al. 2013). Assuming that an antagonist such as [^{3}H]-DIP binds all hMOR conformations with the same affinity, and that within the agonist concentration range explored [^{3}H]-DAMGO only binds to a pool of receptors in a high affinity state, the proportion of receptors in a high affinity state can be estimated. Thus, the proportion of high-affinity-state receptors for agonists was lower in Pp-hMOR (7.5%) compared to SH-hMOR (50%). Moreover, a higher proportion of sites in the low affinity state is consistent with the higher apparent Ki values of the agonist (DAMGO and MOR) measured in the agonist concentration range in competition assay with [^{3}H]-DIP, compared to the Ki values measured in the so-called homologous competition assay. These discrepancies between the binding properties of a receptor coupled to G-proteins in its natural environment (as in SH-SY5Y) and those observed with Pp-hMOR may be explained by the composition of *P. pastoris* membranes. Specifically, these membranes appear to favour the low-affinity-state receptors conformations.

Myriad evidence about the study of G-protein-coupled receptors indicate that G-proteins stabilise high-affinity-state conformations (Hilger, Masureel et al. 2018). Thus, we analysed the [^{35}S]-GTPγS binding and the effect of the addition of GTPγS on *P. pastoris* membrane binding parameters. The [^{35}S]-GTPγS assay measures the level of G-protein activation following agonist occupation of a GPCR by determining the binding of the non-hydrolysable analog [^{35}S]-GTPγS to Gα subunits (Harrison and Traynor 2003). As expected, there was a shift in affinity for SH-hMOR membranes (Fig. 3B and 3D) when GTPγS was added. The affinity for DAMGO was lowered by a factor 3 after GTPγS addition (K_D reduced from 1.07 ± 0.07 to 3.6 ± 0.8 nM). GTPγS addition did not affect the affinity of the antagonist [^{3}H]-DIP (data not shown). In Pp-hMOR, [^{35}S]-GTPγS binding was not stimulated with DAMGO (Fig. 3A). The uncoupling of Pp-hMOR with endogenous G-proteins was confirmed with the absence of effect when GTPγS was added in the saturation-binding buffer (Fig. 3C). In *P. pastoris,* two GPCR systems coexist; they are orthologs of genes found in *S. cerevisiae*. The pheromone response pathway system comprises two receptors, Ste2 and Ste3, and one Gα protein, Gpa1, whereas the glucose-sensing GPCR system comprises one receptor, Gpr1, and one Gα protein, Gpa2 (Versele, Lemaire et al. 2001; Nazarko, Futej et al. 2008). Thus, even in the presence of these endogenous systems, interaction of Gpa1 or Gpa2 with recombinant receptors in *P. pastoris* is inefficient. We extensively attempted to reconstitute G-protein coupling using purified G-proteins and standard reconstitution procedures, but we failed to obtain any positive results (data not shown). The [^{35}S]-GTPγS binding stimulation assay with an agonist is critical because uncoupling of G-protein from receptors does not necessarily affect binding constants. Indeed, in mouse brain, binding of the mu opioid

receptor agonist [^{3}H]-[Dmt1]-DALDA was not affected by the addition of the uncoupling agent Gpp(NH)p (Zhao, Qian et al. 2003).

Sterol composition plays an important role in membrane organisation and function of G-protein coupled receptors (Gimpl, Burger et al. 1997). Ergosterol, the principal fungal sterol, differs from cholesterol because it has an additional methyl group at C24 in the side chain and two additional double bonds, one at C7 in ring B of the nucleus and the other at C22 in the side chain. Ergosterol promotes the formation of lipid domains more that cholesterol in liposomes composed of 1,2-dipalmitoyl-sn-glycero-3-phosphocholine (DPPC)/dioleoyl phosphocholine. Lipid domains are believed to be essential for the maintenance of membrane structure and function (Arora, Raghuraman et al. 2004). In artificial membranes, cholesterol lengthens the saturated and unsaturated lipid chains, whereas ergosterol make the membrane thinner (Hung, Lee et al. 2016).

Ergosterol depletion with MβCD in Pp-hMOR cell membranes did not affect [^{3}H]-DAMGO binding parameters (K_D and B_{max}) in the tested concentration range (Table 3; Fig. 4). Ki values determined by measuring [^{3}H]-DAMGO displacement by DAMGO or MOR were higher. These data suggest that MβCD treatment induced the occurrence of lower-affinity receptor conformations. When cholesterol was added after ergosterol-depletion or when cholesterol was loaded in ergosterol-containing natural membranes, there was an increased affinity of DAMGO (K_D, Ki) and MOR (Ki) for Pp-hMOR; it reached nanomolar values (Table 3; Fig. 4). Moreover, the number of receptors detected with DAMGO binding increased by a factor three. Thus, the addition of cholesterol by MβCD apparently generated a more hMOR in a high affinity state than observed in *P. pastoris* ergosterol-containing membranes. These

experiments also demonstrated that the re-distribution between different conformational states promoted by a sterol species content is reversible.

Several investigations suggested that cholesterol is required to generate the high-affinity hMOR state. In Sc-hMOR membranes, cholesterol complementation restores [^{3}H]-DAMGO binding (Lagane, Gaibelet et al. 2000). When hMOR is uncoupled by addition of a G-protein uncoupling agent to CHO-hMOR membranes (Gaibelet, Millot et al. 2008), cholesterol depletion or ergosterol complementation decreases [^{3}H]-DAMGO affinity. The addition of cholesterol to depleted membranes restore the initial affinity level. In hMOR-expressing HEK cells, there is a decrease in [^{3}H]-DAMGO-labelled receptors after cholesterol depletion. These data indicate a loss of mu-opioid receptors in a high affinity state (Levitt, Clark et al. 2009). Taken together, these results show that G-proteins are not required to observe agonist binding. Furthermore, cholesterol favours and stabilises high-affinity-state conformations irrespective of the presence of G-proteins.

Cholesterol-depletion effects are opioid-subtype dependent because no change in agonist binding constants and B_{max} are observed for the delta opioid-Gαi1 fusion protein (Brejchova, Sykora et al. 2011) expressed in HEK cells. An inverse behaviour is observed for the kappa-opioid receptor expressed in CHO, where agonist affinity increases after cholesterol depletion (Xu, Yoon et al. 2006). In other membrane-containing GPCRs, various agonist binding responses are observed after cholesterol depletion with MβCD. These data include loss of agonist binding for oxytocin and cholecystokinin receptors (Gimpl, Burger et al. 1997), lack of effect in agonist binding constants and B_{max} values for A2a receptor (McGraw, Yang et al. 2019) and TRH receptors (Ostasov, Bourova et al. 2007). MβCD-mediated membrane cholesterol removal can also affect near and downstream GPCR

signalling: reduction of downstream signalling activity of the adenosine A_{2a} receptor as measured via cAMP accumulation (McGraw, Yang et al. 2019), intracellular calcium responses to SDF-1α, receptor internalisation impairment for CXCR4 receptor (Nguyen and Taub 2002) and increased G-protein-activating metarhodopsin II in bovine rod disk membranes (Niu, Mitchell et al. 2002). Sterol effects are not limited to cholesterol. Thus, the STE2 receptor from *S. cerevisiae* normally functions in an ergosterol-membrane-containing environment. In an engineered cholesterol-producing yeast strain, the α-factor specific ligand induces the activation of genes required for mating with lower efficacy (Morioka, Shigemori et al. 2013).

Collectively, these data illustrate the role of sterols in GPCR function, from the binding of drugs to downstream signalling. The identification and characterisation of driving forces that are involved in the cholesterol requirement for GPCR function are well documented (Gimpl 2016). For the mu opioid receptor, direct sterol binding was identified after analysis of X-ray diffraction phase diagram of GPCR crystals; one cholesterol was found to bind to residues of TM6 and TM7, including the connecting loop region ECL3 at the extracellular side of the receptor (Manglik, Kruse et al. 2012; Huang, Manglik et al. 2015; Gimpl 2016). This direct interaction does not exclude a more distant effect of cholesterol.

In conclusion, our study highlights the importance of considering the influence of membrane composition on the effectiveness of active conformations of membrane proteins. Accordingly, for structural investigations of active receptor structures, it is crucial to determine the pharmacological profile of a heterologous recombinant receptor and its specific lipid requirement. We demonstrated that sterols in *P. pastoris* could play a direct role in hMOR conformation and thus modify the proportion of high- versus low-affinity-conformation states. Specifically, cholesterol

has a greater ability to stabilise the high-affinity hMOR conformation state compared to ergosterol. Therefore, to explore active receptor structures, modification of membrane composition may be considered as a useful strategy to manipulate *P. pastoris* as a biotechnical tool.

Competing interest statement

The authors declare no conflict of interest.

Fig. 1

In *Pichia pastoris*, hMOR number was higher when detection was performed with [^{3}H]-DIP compared to [^{3}H]-DAMGO.

(A) Saturation curve produced with [^{3}H]-DIP that assessed total and non-specific binding with unlabelled DIP.

(B) Saturation curve produced with [^{3}H]-DAMGO (total binding) and non-specific binding with unlabelled DAMGO.

[^{3}H]-DIP detected high- and low-affinity receptor states, while [^{3}H]-DAMGO only detected high-affinity states in the tested concentration range.

Fig. 2

Pp-hMOR displayed low affinity binding for the agonists morphine (MOR) and DAMGO.

Competition binding experiments in membranes prepared from Pp-hMOR (A, B) and SH-hMOR (C, D). Unlabelled ligands were added at increasing concentrations in competition with [^{3}H]-DIP (A, C) and [^{3}H]-DAMGO (B, D).

Each data point represents the mean ± SEM for triplicate measurements.

Fig. 3

Pp-hMOR were not coupled with endogenous G-proteins.

In Pp-hMOR, the agonist DAMGO was unable to stimulate (flat curve) [^{35}S]-GTPγS binding (A), and the addition of the uncoupling agent GTPγS had no effect on K_D (C). In SH-hMOR, significant variations in Ki (B), B_{max} and K_D (D) were observed following GTPγS addition.

Fig. 4

Pp-hMOR agonist saturation binding curves were modified following the addition of MβCD.

Pp-hMOR membranes were either depleted of ergosterol with MβCD, loaded with cholesterol after depletion or loaded with cholesterol without ergosterol depletion.

Table 1

Comparison of binding and displacement studies from SH-hMOR and Pp-hMOR.

Saturation binding experiments were performed on membranes using [3H]-DAMGO and [^{3}H]-DIP. Unlabelled DAMGO and DIP were used to determine non-specific binding. Expression levels (B_{max}, pmol/mg membrane proteins) were determined from saturation curves. Notes: [a] data obtained from (Talmont, Mouledous et al. 2014); ND, not determined

Table 2

Comparison of competition studies from SH-hMOR and Pp-hMOR.

Displacement experiments were performed using [^{3}H]-DAMGO and [^{3}H]-DIP. Each Ki value, given in nM, represents the mean ± SEM of three experiments performed in duplicate. Abbreviations: DIP, diprenorphine; NAL, naloxone, MOR, morphine, β-FNA, β-funaltexamine.

Table 3

Effect of methyl-β-cyclodextrin (MβCD) and cholesterol treatment on the K_D value of [^{3}H]-DAMGO binding and K_i values of DAMGO and morphine binding to Pp-hMOR.

Membranes, prepared by ultracentrifugation, were incubated with MβCD (depleted) or depleted and then loaded with a cholesterol-MβCD (CH-MβCD) complex (depleted-loaded). Membranes were also directly loaded with CH-MβCD (loaded). Each value represents the mean ± SEM of three experiments performed in duplicate.

References

Alt, A., M. J. Clark, et al. (2002). "Mu and Delta opioid receptors activate the same G proteins in human neuroblastoma SH-SY5Y cells." Br J Pharmacol **135**(1): 217-225.

Arora, A., H. Raghuraman, et al. (2004). "Influence of cholesterol and ergosterol on membrane dynamics: a fluorescence approach." Biochem Biophys Res Commun **318**(4): 920-926.

Bertheleme, N., S. Singh, et al. (2015). "Heterologous expression of G-protein-coupled receptors in yeast." Methods Enzymol **556**: 141-164.

Brejchova, J., J. Sykora, et al. (2011). "Fluorescence spectroscopy studies of HEK293 cells expressing DOR-Gi1alpha fusion protein; the effect of cholesterol depletion." Biochim Biophys Acta **1808**(12): 2819-2829.

Cui, X., A. Yeliseev, et al. (2013). "Ligand interaction, binding site and G protein activation of the mu opioid receptor." Eur J Pharmacol **702**(1-3): 309-315.

Darby, R. A., S. P. Cartwright, et al. (2012). "Which yeast species shall I choose? Saccharomyces cerevisiae versus Pichia pastoris (review)." Methods Mol Biol **866**: 11-23.

Gabilondo, A. M., J. J. Meana, et al. (1994). "mu-Opioid receptor and alpha 2-adrenoceptor agonist binding sites in the postmortem brain of heroin addicts." Psychopharmacology (Berl) **115**(1-2): 135-140.

Gabilondo, A. M., J. J. Meana, et al. (1995). "Increased density of mu-opioid receptors in the postmortem brain of suicide victims." Brain Res **682**(1-2): 245-250.

Gaibelet, G., E. Meilhoc, et al. (1999). "Nonselective coupling of the human mu-opioid receptor to multiple inhibitory G-protein isoforms." Eur J Biochem **261**(2): 517-523.

Gaibelet, G., C. Millot, et al. (2008). "Cholesterol content drives distinct pharmacological behaviours of micro-opioid receptor in different microdomains of the CHO plasma membrane." Mol Membr Biol **25**(5): 423-435.

Gimpl, G. (2016). "Interaction of G protein coupled receptors and cholesterol." Chem Phys Lipids **199**: 61-73.

Gimpl, G., K. Burger, et al. (1997). "Cholesterol as modulator of receptor function." Biochemistry **36**(36): 10959-10974.

Granier, S., A. Manglik, et al. (2012). "Structure of the delta-opioid receptor bound to naltrindole." Nature **485**(7398): 400-404.

Harrison, C. and J. R. Traynor (2003). "The [35S]GTPgammaS binding assay: approaches and applications in pharmacology." Life Sci **74**(4): 489-508.

Hartmann, L., V. Kugler, et al. (2016). "Expression of Eukaryotic Membrane Proteins in Pichia pastoris." Methods Mol Biol **1432**: 143-162.

Hilger, D., M. Masureel, et al. (2018). "Structure and dynamics of GPCR signaling complexes." Nat Struct Mol Biol **25**(1): 4-12.

Hino, T., T. Arakawa, et al. (2012). "G-protein-coupled receptor inactivation by an allosteric inverse-agonist antibody." Nature **482**(7384): 237-240.

Huang, W., A. Manglik, et al. (2015). "Structural insights into micro-opioid receptor activation." Nature **524**(7565): 315-321.

Hung, W. C., M. T. Lee, et al. (2016). "Comparative Study of the Condensing Effects of Ergosterol and Cholesterol." Biophys J **110**(9): 2026-2033.

Hutchings, C. J., M. Koglin, et al. (2010). "Therapeutic antibodies directed at G protein-coupled receptors." MAbs **2**(6): 594-606.

Koehl, A., H. Hu, et al. (2018). "Structure of the micro-opioid receptor-Gi protein complex." Nature **558**(7711): 547-552.

Lagane, B., G. Gaibelet, et al. (2000). "Role of sterols in modulating the human mu-opioid receptor function in Saccharomyces cerevisiae." J Biol Chem **275**(43): 33197-33200.

Levitt, E. S., M. J. Clark, et al. (2009). "Differential effect of membrane cholesterol removal on mu- and delta-opioid receptors: a parallel comparison of acute and chronic signaling to adenylyl cyclase." J Biol Chem **284**(33): 22108-22122.

Manglik, A., A. C. Kruse, et al. (2012). "Crystal structure of the micro-opioid receptor bound to a morphinan antagonist." Nature **485**(7398): 321-326.

McGraw, C., L. Yang, et al. (2019). "Membrane cholesterol depletion reduces downstream signaling activity of the adenosine A2a receptor." Biochim Biophys Acta Biomembr.

Mollereau, C., M. Parmentier, et al. (1994). "ORL1, a novel member of the opioid receptor family. Cloning, functional expression and localization." FEBS Lett **341**(1): 33-38.

Morioka, S., T. Shigemori, et al. (2013). "Effect of sterol composition on the activity of the yeast G-protein-coupled receptor Ste2." Appl Microbiol Biotechnol **97**(9): 4013-4020.

Mouledous, L., J. Neasta, et al. (2005). "Long-term morphine treatment enhances proteasome-dependent degradation of G beta in human neuroblastoma SH-SY5Y cells: correlation with onset of adenylate cyclase sensitization." Mol Pharmacol **68**(2): 467-476.

Nazarko, V. Y., K. O. Futej, et al. (2008). "Differences in glucose sensing and signaling for pexophagy between the baker's yeast Saccharomyces cerevisiae and the methylotrophic yeast Pichia pastoris." Autophagy **4**(3): 381-384.

Nguyen, D. H. and D. Taub (2002). "CXCR4 function requires membrane cholesterol: implications for HIV infection." J Immunol **168**(8): 4121-4126.

Niu, S. L., D. C. Mitchell, et al. (2002). "Manipulation of cholesterol levels in rod disk membranes by methyl-beta-cyclodextrin: effects on receptor activation." J Biol Chem **277**(23): 20139-20145.

Ostasov, P., L. Bourova, et al. (2007). "Disruption of the plasma membrane integrity by cholesterol depletion impairs effectiveness of TRH receptor-mediated signal transduction via G(q)/G(11)alpha proteins." J Recept Signal Transduct Res **27**(5-6): 335-352.

Salom, D., P. S. Padayatti, et al. (2013). "Crystallization of G protein-coupled receptors." Methods Cell Biol **117**: 451-468.

Sarramegna, V., I. Muller, et al. (2005). "Solubilization, purification, and mass spectrometry analysis of the human mu-opioid receptor expressed in Pichia pastoris." Protein Expr Purif **43**(2): 85-93.

Sarramegna, V., F. Talmont, et al. (2003). "Heterologous expression of G-protein-coupled receptors: comparison of expression systems from the standpoint of large-scale production and purification." Cell Mol Life Sci **60**(8): 1529-1546.

Sarramegna, V., F. Talmont, et al. (2002). "Green fluorescent protein as a reporter of human mu-opioid receptor overexpression and localization in the methylotrophic yeast Pichia pastoris." J Biotechnol **99**(1): 23-39.

Shimamura, T., M. Shiroishi, et al. (2011). "Structure of the human histamine H1 receptor complex with doxepin." Nature **475**(7354): 65-70.

Sounier, R., C. Mas, et al. (2015). "Propagation of conformational changes during mu-opioid receptor activation." Nature **524**(7565): 375-378.

Suh, S. O., M. Blackwell, et al. (2006). "Phylogenetics of Saccharomycetales, the ascomycete yeasts." Mycologia **98**(6): 1006-1017.

Talmont, F., L. Mouledous, et al. (2014). "Solubilization and reconstitution of the mu-opioid receptor expressed in human neuronal SH-SY5Y and CHO cells." Peptides **55**: 79-84.

Talmont, F., S. Sidobre, et al. (1996). "Expression and pharmacological characterization of the human mu-opioid receptor in the methylotrophic yeast Pichia pastoris." FEBS Lett **394**(3): 268-272.

Thal, D. M., Z. Vuckovic, et al. (2018). "Recent advances in the determination of G protein-coupled receptor structures." Curr Opin Struct Biol **51**: 28-34.

Thompson, A. A., W. Liu, et al. (2012). "Structure of the nociceptin/orphanin FQ receptor in complex with a peptide mimetic." Nature **485**(7398): 395-399.

Thorsen, T. S., R. Matt, et al. (2014). "Modified T4 Lysozyme Fusion Proteins Facilitate G Protein-Coupled Receptor Crystallogenesis." Structure **22**(11): 1657-1664.

Versele, M., K. Lemaire, et al. (2001). "Sex and sugar in yeast: two distinct GPCR systems." EMBO Rep **2**(7): 574-579.

Wu, E. H. and Y. H. Wong (2005). "Activation of delta-, kappa-, and mu-opioid receptors induces phosphorylation of tuberin in transfected HEK 293 cells and native cells." Biochem Biophys Res Commun **334**(3): 838-844.

Wu, H., D. Wacker, et al. (2012). "Structure of the human kappa-opioid receptor in complex with JDTic." Nature **485**(7398): 327-332.

Xu, W., S. I. Yoon, et al. (2006). "Localization of the kappa opioid receptor in lipid rafts." J Pharmacol Exp Ther **317**(3): 1295-1306.

Zhao, G. M., X. Qian, et al. (2003). "Comparison of [Dmt1]DALDA and DAMGO in binding and G protein activation at mu, delta, and kappa opioid receptors." J Pharmacol Exp Ther **307**(3): 947-954.

Table 1

	Pp-hMOR		SH-hMOR	
	[^{3}H]-DIP	[^{3}H]-DAMGO	[^{3}H]-DIP	[^{3}H]-DAMGO
K_D (nM)	2.4 ± 0.3	7.4 ± 1.5	0.34 ± 0.07[a]	1.06 ± 0.07[a]
B_{max} (pmol/mg)	0.4 ± 0.1	0.031 ± 0.003	25.37 ± 1.57[a]	13.65 ± 0.20[a]
K_D (nM) + GTPγS	ND	ND	ND	3.6 ± 0.8

Table 2

	Pp-hMOR		SH-hMOR	
Competitor	[^{3}H]-DIP Ki (nM)	[^{3}H]-DAMGO Ki (nM)	[^{3}H]-DIP Ki (nM)	[^{3}H]-DAMGO Ki (nM)
DIP	3.1 ± 0.7	1.6 ± 0.3	0.12 ± 0.01	0.14 ± 0.02
NAL	34 ± 2	34 ± 10	1.7 ± 0.5	2.0 ± 0.1
DAMGO	107 ± 21	15.7 ± 2.3	1.6 ± 0.2	0.7 ± 0.1
MOR	107 ± 10	27 ± 7	5.1 ± 0.5	3.4 ± 0.4
β-FNA	21 ± 4	0.7 ± 0.2	1.1 ± 0.4	0.8 ± 0.1

Table 3

Ligand	Initial	Depleted	Depleted-loaded	Loaded
DAMGO K_D (nM)	7.4 ± 1.5	10.6 ± 1.4	4.6 ± 0.9	2.3 ± 0.4
DAMGO Ki(nM)	15.7 ± 2.3	141 ± 68	4.1 ± 1.5	3.2 ± 0.7
MOR Ki (nM)	27 ± 7	133 ± 39	31 ± 7	25 ± 9

Figure 1

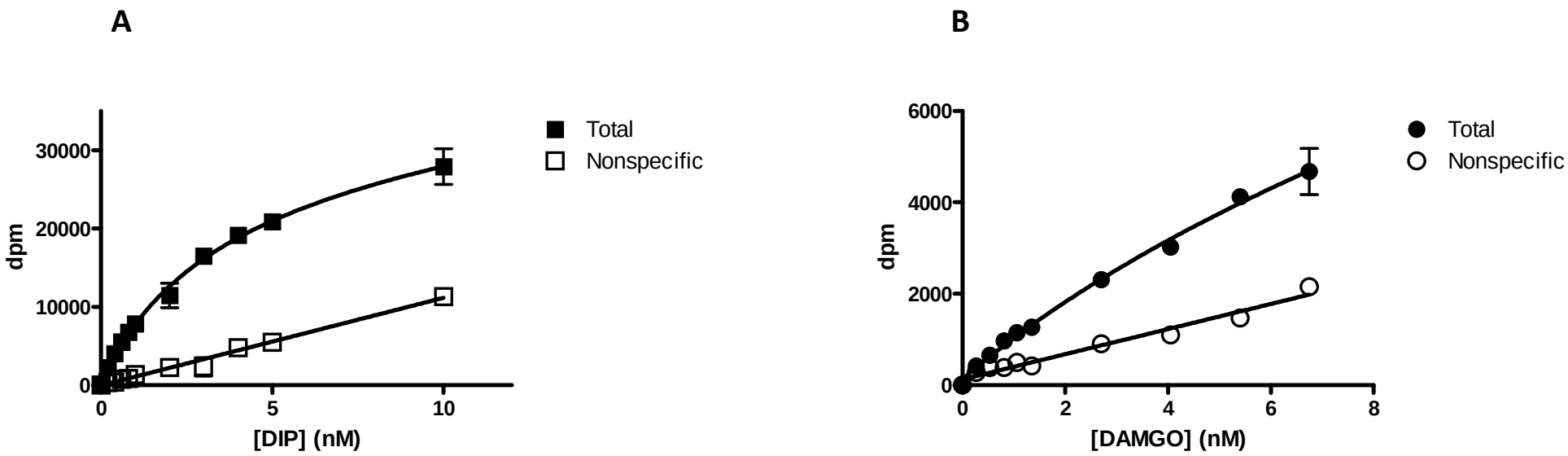
A
dpm
30000
20000
10000
0
0
5
10
[DIP] (nM)
Total
Nonspecific
B
dpm
6000
4000
2000
0
0
2
4
6
8
[DAMGO] (nM)
Total
Nonspecific

Figure 2

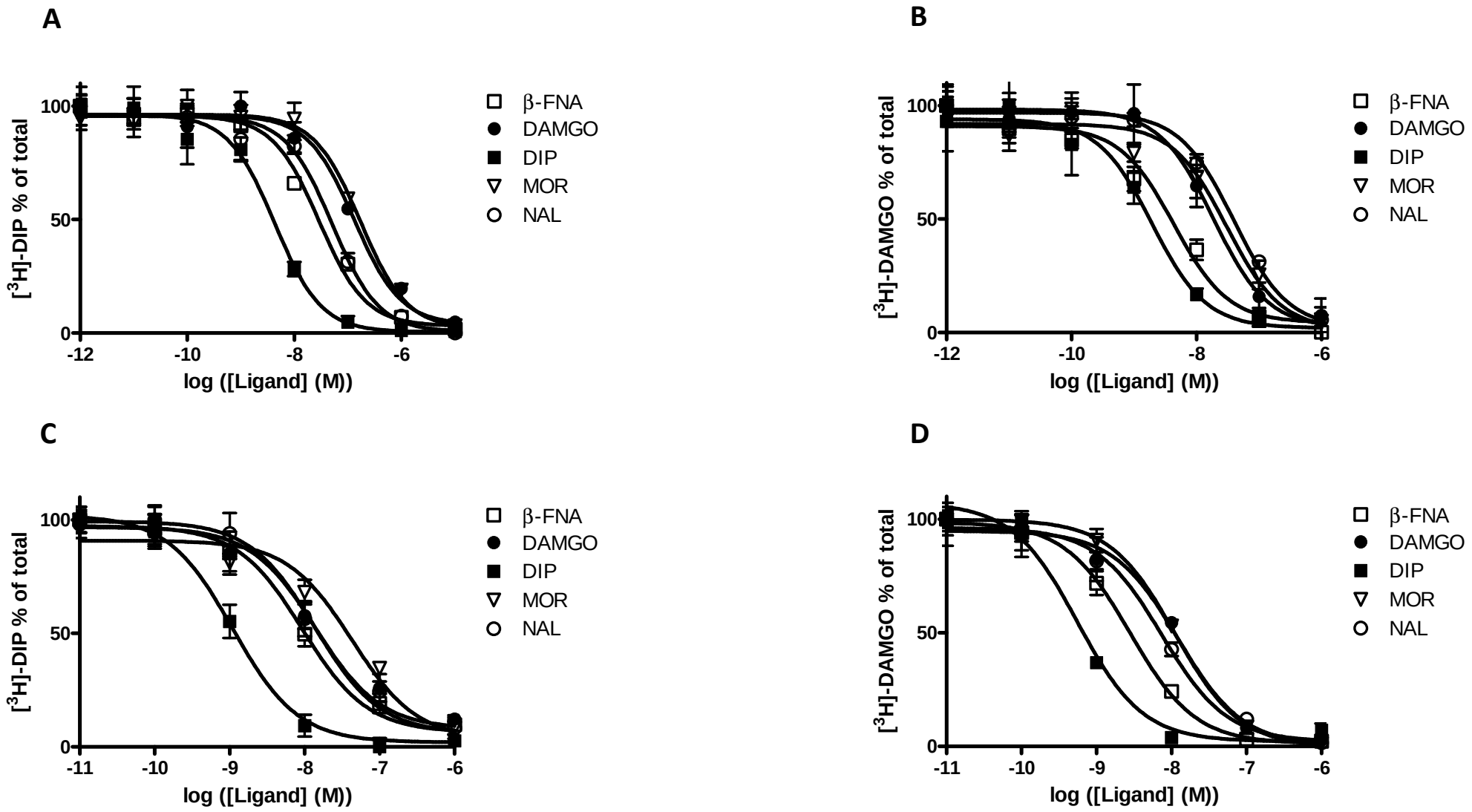
A
B
C
D
β-FNA
DAMGO
DIP
MOR
NAL
[3H]-DIP % of total
[3H]-DAMGO % of total
log ([Ligand] (M))
100
50
0
-12
-10
-8
-6
-11
-9
-7

Figure 3

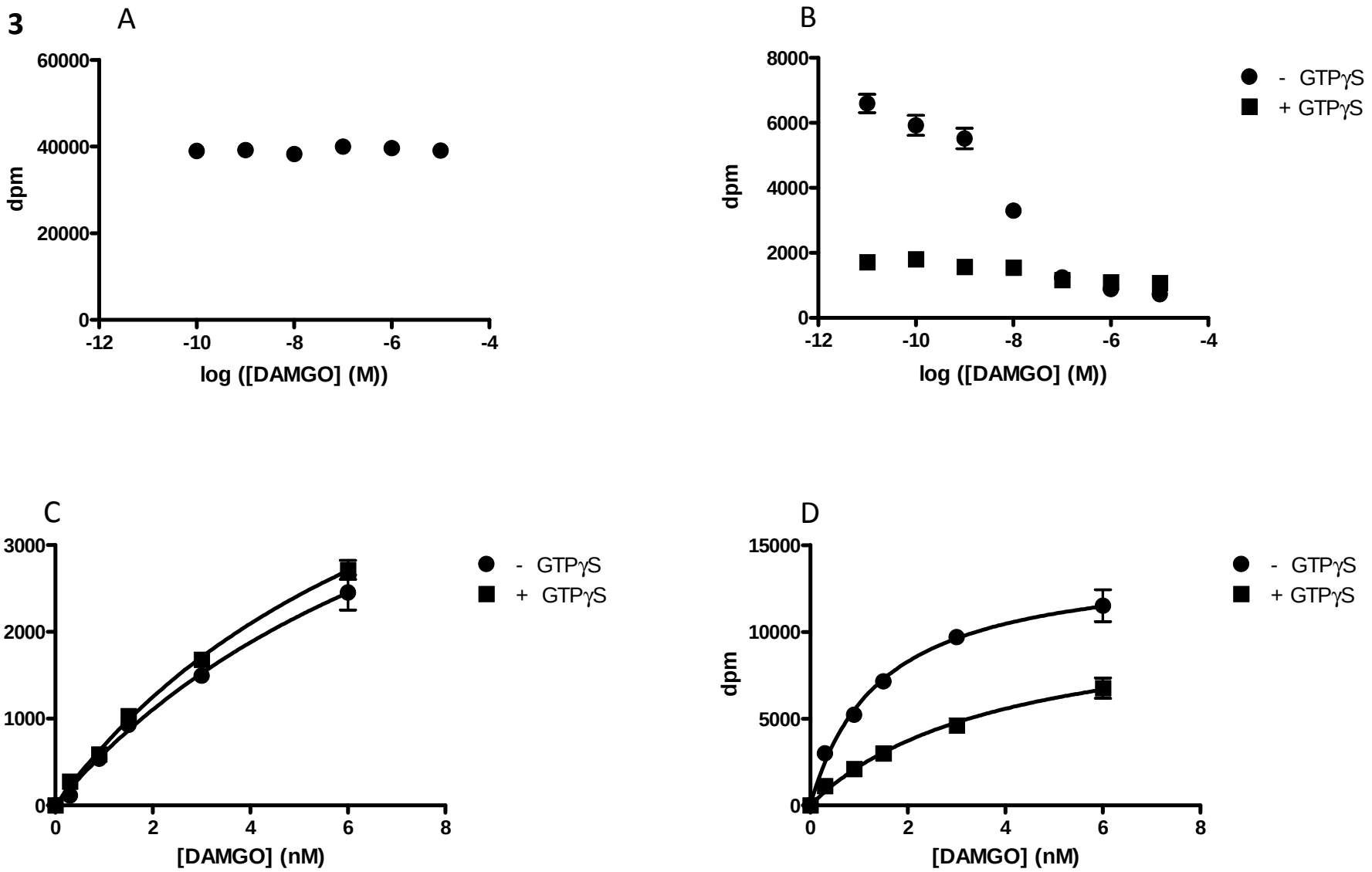
A
60000
40000
20000
0
dpm
-12
-10
-8
-6
-4
log ([DAMGO] (M))
B
8000
6000
4000
2000
0
dpm
-12
-10
-8
-6
-4
log ([DAMGO] (M))
- GTPγS
+ GTPγS
C
3000
2000
1000
0
dpm
0
2
4
6
8
[DAMGO] (nM)
- GTPγS
+ GTPγS
D
15000
10000
5000
0
dpm
0
2
4
6
8
[DAMGO] (nM)
- GTPγS
+ GTPγS

Figure 4

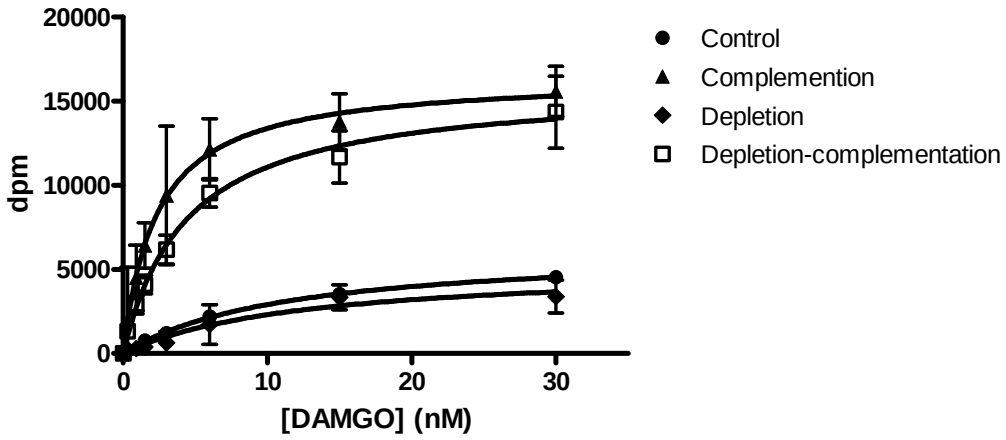
20000
15000
10000
5000
0
dpm
0
10
20
30
[DAMGO] (nM)
Control
Complemention
Depletion
Depletion-complementation

Highlights

The agonist DAMGO binds mu opioid receptors overexpressed in *Pichia pastoris*.

Cholesterol is an essential component to ensure the functioning of receptors.

Conformational states promoted by a sterol species content is reversible.